\



Theoretical investigation of ferromagnetic resonance in a ferromagnetic thin film with external stress anisotropy

Jieyu Zhou(周婕妤), Jianhong Rong(荣建红), Huan Wang(王焕), Guohong Yun(云国宏), Yanan Wang(王娅男), and Shufei Zhang(张舒飞)

Citation: Chin. Phys. B, 2022, 31 (**1**): 017601. DOI: 10.1088/1674-1056/ac1b86
Journal homepage: http://cpb.iphy.ac.cn; http://iopscience.iop.org/cpb

What follows is a list of articles you may be interested in

Controlled vapor growth of 2D magnetic Cr_2Se_3 and its magnetic proximity effect in heterostructures

Danliang Zhang(张丹亮), Chen Yi(易琛), Cuihuan Ge(葛翠环), Weining Shu(舒维宁), Bo Li(黎博), Xidong Duan(段曦东), Anlian Pan(潘安练), and Xiao Wang(王笑)

Chin. Phys. B, 2021, 30 (**9**): 097601. DOI: 10.1088/1674-1056/ac0cd9

Effect of interface magnetization depinning on the frequency shift of ferromagnetic and spin wave resonance in YIG/GGG films

Fanqing Lin(林凡庆), Shouheng Zhang(张守珩), Guoxia Zhao(赵国霞), Hongfei Li(李洪飞), Weihua Zong(宗卫华), Shandong Li(李山东)

Chin. Phys. B, 2020, 29 (**6**): 067601. DOI: 10.1088/1674-1056/ab8dac

Large tunable FMR frequency shift by magnetoelectric coupling in oblique-sputtered $Fe_{52.5}Co_{22.5}B_{25.0}$/PZN-PT multiferroic heterostructure

Zhi-Peng Shi(时志鹏), Xiao-Min Liu(刘晓敏), Shan-Dong Li(李山东)

Chin. Phys. B, 2017, 26 (**9**): 097601. DOI: 10.1088/1674-1056/26/9/097601

Magnetic transition behavior of perovskite manganites $Nd_{0.5}Sr_{0.3}Ca_{0.2}MnO_3$ polycrystalline

Ru Xing(邢茹), Su-Lei Wan(万素磊), Wen-Qing Wang(王文清), Lin Zheng(郑琳), Xiang Jin(金香), Min Zhou(周敏), Yi Lu(鲁毅), Jian-Jun Zhao(赵建军)

Chin. Phys. B, 2016, 25 (**4**): 047601. DOI: 10.1088/1674-1056/25/4/047601

An electron spin resonance study of Eu doping effect in $La_{4/3}Sr_{5/3}Mn_2O_7$ single crystal

He Li-Min, Ji Yu, Wu Hong-Ye, Xu Bao, Sun Yun-Bin, Zhang Xue-Feng, Lu Yi, Zhao Jian-Jun

Chin. Phys. B, 2014, 23 (**7**): 077601. DOI: 10.1088/1674-1056/23/7/077601

Theoretical investigation of ferromagnetic resonance in a ferromagnetic thin film with external stress anisotropy

Jieyu Zhou(周婕妤)[1], Jianhong Rong(荣建红)[1,†], Huan Wang(王焕)[2], Guohong Yun(云国宏)[1,3], Yanan Wang(王娅男)[1], and Shufei Zhang(张舒飞)[1]

[1] *Inner Mongolia Key Laboratory of Nanoscience and Nanotechnology and School of Physical Science and Technology, Inner Mongolia University, Hohhot* 010021, *China*

[2] *College of Science, Inner Mongolia Agricultural University, Hohhot* 010018, *China*

[3] *College of Physics and Electronic Information, Inner Mongolia Normal University, Hohhot* 010022, *China*

(Received 11 May 2021; revised manuscript received 22 July 2021; accepted manuscript online 7 August 2021)

We use the ferromagnetic resonance (FMR) method to study the properties of ferromagnetic thin film, in which external stress anisotropy, fourfold anisotropy and uniaxial anisotropy are considered. The analytical expressions of FMR frequency, linewidth and the imaginary part of magnetic susceptibility are obtained. Our results reveal that the FMR frequency and the imaginary part of magnetic susceptibility are distinctly enhanced, and the frequency linewidth or field linewidth are broadened due to a strong external stress anisotropy field. The hard-axis and easy-axis components of magnetization can be tuned significantly by controlling the intensity and direction of stress and the in-plane uniaxial anisotropy field.

Keywords: ferromagnetic resonance, external stress anisotropy, fourfold anisotropy, uniaxial anisotropy

PACS: 76.50.+g, 75.70.Ak, 75.30.Gw **DOI:** 10.1088/1674-1056/ac1b86

1. Introduction

Recently, several methods have been used to research the single, bilayers and multilayers of ferromagnetic film, such as ferromagnetic resonance (FMR)[1–5] and Brillouin light scattering.[6–8] Ferromagnetic resonance is a powerful tool for quantitative determination of the properties of magnetic materials, such as magnetic anisotropies and relaxation,[9,10] magnetic coupling,[11,12] linewidth,[13–16] and others. However, in these studies, most of the investigations only take into account interlayer coupling and exchange bias.[17–23] Reports on the theoretical analysis of stress anisotropy in ferromagnetic thin film are scarcer. In fact, the controllable stress plays an important role in the FMR, which can change the properties of magnetic materials.[24] To date, although there are a few reports on stress,[25–29] the effects of the intensity and direction of external stress anisotropy on FMR are not yet thoroughly understood in a ferromagnetic thin film that includes fourfold anisotropy and uniaxial anisotropy. The motivation of the present work is to theoretically investigate the ferromagnetic resonance properties of ferromagnetic thin film with an external stress anisotropy field in detail. Therefore, in this paper, we report tuning of the FMR frequency, the linewidth and the imaginary part of magnetic susceptibility by alternating the intensity and direction of the external stress anisotropy. Also, the effect of the direction of in-plane uniaxial anisotropy is discussed in this system. Our objective is to further understand magnetic dynamic properties and show how to obtain high and controllable FMR frequency.

2. Theoretical model and calculation procedure

For the quantitative analysis, we have employed a model that takes into account fourfold anisotropy, uniaxial anisotropy and external stress anisotropy. The film plane lies in the x–y plane, while the z axis is normal to it, as shown in Fig. 1. The polar and azimuthal angles of the applied magnetic field H in the corresponding spherical coordinate system are θ_H and φ_H. Similarly, the magnetization M and external stress anisotropy field H_σ are θ and φ, θ_σ and φ_σ, respectively. Here, δ is the angle between the in-plane uniaxial anisotropy and the x axis positive direction. In this model, the free energy consists of the following five terms: the Zeeman energy, the demagnetizing energy, the in-plane and out-of-plane uniaxial anisotropy energy (with constants $K_{2//}$ and $K_{2\perp}$), the fourfold in-plane and out-of-plane anisotropy energy (with constants $K_{4//}$ and $K_{4\perp}$) and external stress anisotropy energy, so the total free energy per unit area has the following form:

$$\begin{aligned} F \;=\; & -MH[\sin\theta\sin\theta_H\cos(\varphi-\varphi_H)+\cos\theta\cos\theta_H] \\ & -2\pi M^2\sin^2\theta+K_{2//}\sin^2\theta\cos^2(\varphi-\delta)\;+K_{2\perp}\sin^2\theta \\ & -\frac{1}{8}K_{4//}(3+\cos 4\varphi)\sin^4\theta-\frac{1}{2}K_{4\perp}\cos^4\theta \\ & -\frac{3}{2}\lambda_s\sigma(\sin\theta_\sigma\cos\varphi_\sigma\sin\theta\cos\varphi \\ & +\sin\theta_\sigma\sin\varphi_\sigma\sin\theta\sin\varphi+\cos\theta_\sigma\cos\theta)^2, \end{aligned} \tag{1}$$

where λ_s and σ are the magnetostriction coefficient and stress intensity; for simplicity, we assume the magnetostriction of the film is isotropic.

†Corresponding author. E-mail: jhrong502@163.com

© 2022 Chinese Physical Society and IOP Publishing Ltd

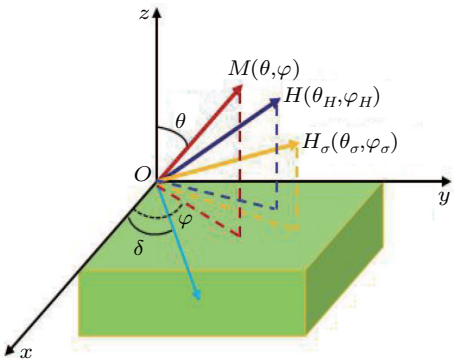


Fig. 1. Sketch of the spherical coordinate system used to describe the orientations of applied field H, magnetization M and external stress anisotropy field H_σ in the ferromagnetic resonance analysis.

The equilibrium position of magnetization is provided by $\partial F/\partial\theta = 0$ and $\partial F/\partial\varphi = 0$. It is observed that the magnetization lying in the plane, $\theta = \theta_H = \theta_\sigma = \pi/2$, is a solution of the equilibrium equation. Thus, the azimuthal angle of magnetization can be determined by the following equation:

$$\begin{aligned} &H\sin(\varphi-\varphi_H)-\frac{1}{2}H_{2n}\sin 2(\varphi-\delta)\\ &+\frac{1}{4}H_{4n}\sin 4\varphi+\frac{3}{4}H_\sigma\sin 2(\varphi-\varphi_\sigma)=0, \end{aligned} \tag{2}$$

where $H_{2n} = 2K_{2//}/M$, $H_{4n} = 2K_{4//}/M$, and $H_\sigma = 2\lambda_s\sigma/M$ are defined as the in-plane uniaxial anisotropy field, fourfold in-plane anisotropy field and external stress anisotropy field, respectively. Then, the FMR frequency can be derived using the Smit and Beljers relation[30]

$$\begin{aligned} \left(\frac{\omega}{\gamma}\right)^2 &= [H\cos(\varphi-\varphi_H)+4\pi M_{\rm eff}-H_{2n}\cos^2(\varphi-\delta)\\ &+\frac{1}{4}H_{4n}(3+\cos 4\varphi)+\frac{3}{2}H_\sigma\cos^2(\varphi-\varphi_\sigma)]\\ &\times[H\cos(\varphi-\varphi_H)-H_{2n}\cos 2(\varphi-\delta)\\ &+H_{4n}\cos 4\varphi+\frac{3}{2}H_\sigma\cos 2(\varphi-\varphi_\sigma)], \end{aligned} \tag{3}$$

where ω is the angular frequency of the microwave field, $4\pi M_{\rm eff} = 4\pi M - H_{2w}$ is the effective magnetization, $H_{2w} = 2K_{2\perp}/M$ is the out-of-plane uniaxial anisotropy field and γ is the magnetogyric ratio. Also, Eq. (3) results in

$$H_{\rm res} = \frac{-(H_1+H_2)+\sqrt{(H_1-H_2)^2+4(\omega/\gamma)^2}}{2\cos(\varphi-\varphi_H)}, \tag{4}$$

where

$$\begin{aligned} H_1 &= 4\pi M_{\rm eff}-H_{2n}\cos^2(\varphi-\delta)+\frac{1}{4}H_{4n}(3+\cos 4\varphi)\\ &+\frac{3}{2}H_\sigma\cos^2(\varphi-\varphi_\sigma), \end{aligned} \tag{5}$$

$$\begin{aligned} H_2 &= -H_{2n}\cos 2(\varphi-\delta)+H_{4n}\cos 4\varphi\\ &+\frac{3}{2}H_\sigma\cos 2(\varphi-\varphi_\sigma). \end{aligned} \tag{6}$$

The linewidth of FMR contains some significant information for the ferromagnetic resonance modes, so the frequency linewidth $\Delta\omega$ and field linewidth ΔH are shown as follows by using the general formula:[17,31]

$$\Delta\omega = \alpha\gamma[2H\cos(\varphi-\varphi_H)+H_1+H_2], \tag{7}$$

$$\Delta H = \frac{2\omega\alpha\,[2H\cos(\varphi-\varphi_H)+H_1+H_2]}{\cos(\varphi-\varphi_H)\sqrt{4\omega^2+\gamma^2(H_1-H_2)^2}}. \tag{8}$$

Here, α is the Gilbert damping coefficient.

As is well known, the experimentally measured absorption part of FMR is related to the imaginary part of magnetic susceptibility.[32] The dynamic susceptibility can be calculated using the following equation:[17]

$$\chi = \frac{\gamma^2\,(F_{\theta\theta}+{\rm i}\omega M\alpha/\gamma)}{(\omega_{\rm r}^2-\omega^2)+{\rm i}\omega\Delta\omega}. \tag{9}$$

At resonant frequency $\omega_{\rm r} = \omega$, and writing χ as $\chi = \chi' - {\rm i}\chi''$, one will get the imaginary part of the dynamic susceptibility

$$\chi'' = \frac{\gamma^2 F_{\theta\theta}}{\omega\Delta\omega} = \frac{\gamma M}{\omega\alpha}\left[\frac{H\cos(\varphi-\varphi_H)+H_1}{2H\cos(\varphi-\varphi_H)+H_1+H_2}\right], \tag{10}$$

which expresses the amplitude of the absorption peak.

2.1. Results and discussion

For comparison with Ref. [33], the corresponding numerical calculation parameters are chosen as follows: $H_{2n} = -0.14$ kOe, $H_{2w} = 3.3$ kOe, $H_{4n} = 0.6$ kOe, $M = 1.7$ kG, $\gamma/2\pi = 2.92$ GHz/kOe, $\alpha = 0.02$. Here, the in-plane uniaxial anisotropy field is along the x axis negative direction. The FMR frequency, frequency linewidth, field linewidth and imaginary part of magnetic susceptibility as a function of the applied magnetic field for different intensities of the external stress anisotropy field are shown in Fig. 2. For simplicity, the directions of the external stress anisotropy field and applied magnetic field are set in a fixed direction ($\varphi_\sigma = \varphi_H = 0°$). It can be seen that the FMR frequency, frequency linewidth and field linewidth are shifted to a higher value when the intensity of the external stress anisotropy field increases [Figs. 2(a)–2(c)]. Moreover, it is observed that there is a critical field H'. According to the energy minimization procedure, $\partial^2F/\partial\theta^2 > 0$ and $\partial^2F/\partial\varphi^2 > 0$, we obtain $H' = -H_{2n}+H_{4n}+(3/2)H_\sigma$, which is very sensitive to the in-plane uniaxial anisotropy field, fourfold in-plane anisotropy field and external stress anisotropy field. When $H < H'$ ($\varphi = \pi$), the FMR frequency, frequency linewidth and field linewidth decrease with the increase in the applied magnetic field for different intensities of the external stress anisotropy field. However, the opposite behavior is seen for $H > H'$ ($\varphi = 0$). It indicates that the direction of magnetization rotates from antiparallel to parallel at the critical field. When the external stress anisotropy field is above 1.0 kOe, the critical field will continue to move to the right side, and similar behavior is observed; we therefore have not shown it here. This is different from previously reported results without an external stress anisotropy field.[33] On the

other hand, one observes that the frequency linewidth presents linear behavior in the weak magnetic field region ($H < H'$) [Fig. 2(b)], which is different from Fig. 2(a). Besides, as seen in Fig. 2(d), as the applied magnetic field increases, the imaginary part of the magnetic susceptibility shows a maximum at the critical field. Nevertheless, when the applied magnetic field exceeds the critical field, the imaginary part of the magnetic susceptibility is exhibited weakly depending on the external stress anisotropy field strength. This is because the in-plane uniaxial, the fourfold in-plane and the external stress anisotropy fields have much smaller values compared to H when $H > H'$, indicating that the imaginary part of the magnetic susceptibility is dominated by the applied magnetic field.

To compare with the no-external stress anisotropy field, the left panel of Fig. 3 only illustrates how the direction of the applied magnetic field affects the FMR frequency f [Fig. 3(a)], magnetic free-energy density F [Fig. 3(b)] and imaginary part of magnetic susceptibility χ'' [Fig. 3(c)]. Here, the intensity of the applied magnetic field is fixed at 3.0 kOe, and the effective magnetization is 18.2 kG in the numerical calculation.[33] The other parameters are the same as in Fig. 2. It is found that the curves are symmetric with respect to the $\langle 010 \rangle$ direction.

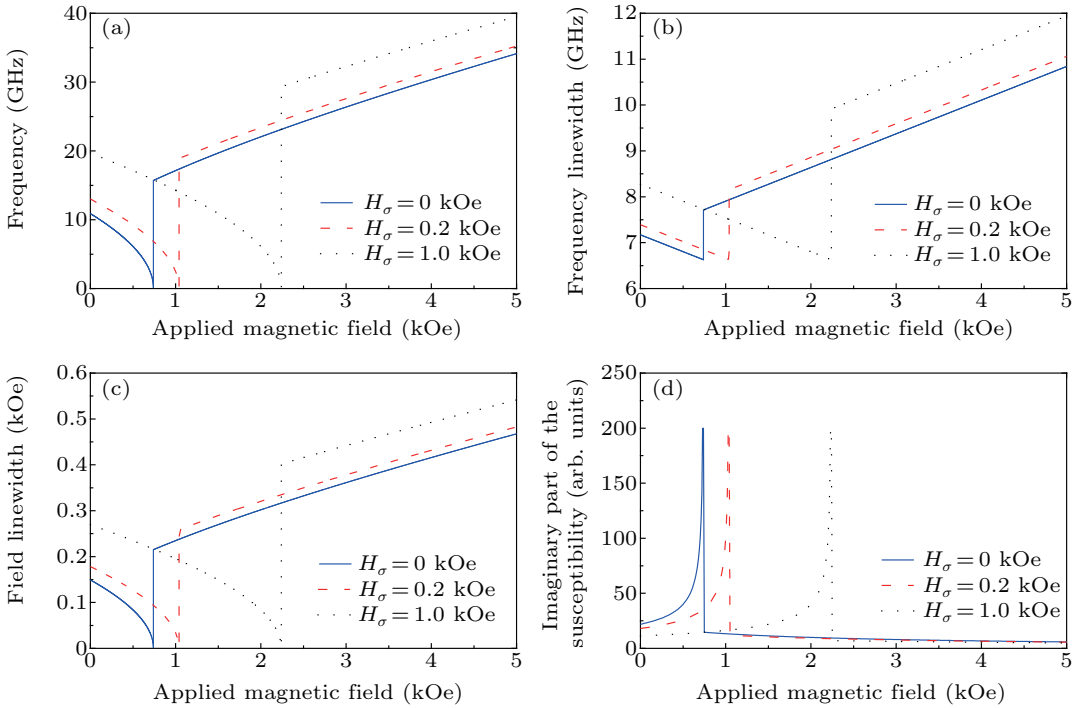


Fig. 2. Applied magnetic field dependence of (a) FMR frequency, (b) frequency linewidth, (c) field linewidth, and (d) imaginary part of magnetic susceptibility for different intensities of external stress anisotropy field.

The middle panel and right panel of Fig. 3 show the angular dependence of the FMR frequency with different directions of the external stress anisotropy field. The intensity of the external stress anisotropy field is fixed at $H_\sigma = 0.2$ kOe (middle panel) and $H_\sigma = 1.0$ kOe (right panel), respectively. As seen in Figs. 3(d), (f), and 3(h), the curves are symmetric about the $\varphi_H = 90^\circ$ for $\varphi_\sigma = 0^\circ, 90^\circ, 180^\circ$. Moreover, two valleys are observed. This indicates that it is hard to magnetize along these two directions. Furthermore, the FMR frequency curves are the same when the external stress anisotropy field is parallel ($\varphi_\sigma = 0^\circ$) or antiparallel ($\varphi_\sigma = 180^\circ$) to the positive direction of the x axis. However, for $\varphi_\sigma = 45^\circ$ and $\varphi_\sigma = 135^\circ$ [Figs. 3(e) and 3(g)], the symmetry is obviously broken. It clearly indicates that the direction of hard magnetization is changed.

To further reveal the effect of the external stress anisotropy field with regard to FMR frequency, the intensity of the external stress anisotropy field is increased up to 1.0 kOe. As shown in the right panel of Fig. 3, the FMR frequencies of the system are maximal and the same at $\varphi_H = 0^\circ$ and $\varphi_H = 180^\circ$, except for $\varphi_\sigma = 90^\circ$. This shows that it is easy to magnetize along these two directions. When we compare the middle panel with the right panel, as we increase the intensity of the external stress anisotropy field, the double valleys are not significant for the directions of the external stress anisotropy field along $\langle 100 \rangle$, $\langle 010 \rangle$ and $\langle \bar{1}00 \rangle$. Outside of these directions, at $\varphi_\sigma = 45^\circ$ and $\varphi_\sigma = 135^\circ$, only one valley can be found in the full range of the angle φ_H in the in-plane configuration. For the $\varphi_\sigma = 90^\circ$ direction, the easy magnetization direction is along $\varphi_H = 90^\circ$. These results demonstrate that the hard and the easy magnetization directions can be controlled by tuning the external stress anisotropy field.

Next, to further investigate the effect of the direction of the in-plane uniaxial anisotropy field on the properties of thin film, we plot the FMR frequency (Fig. 4) and imaginary part of magnetic susceptibility (Fig. 5) as a function of the direction

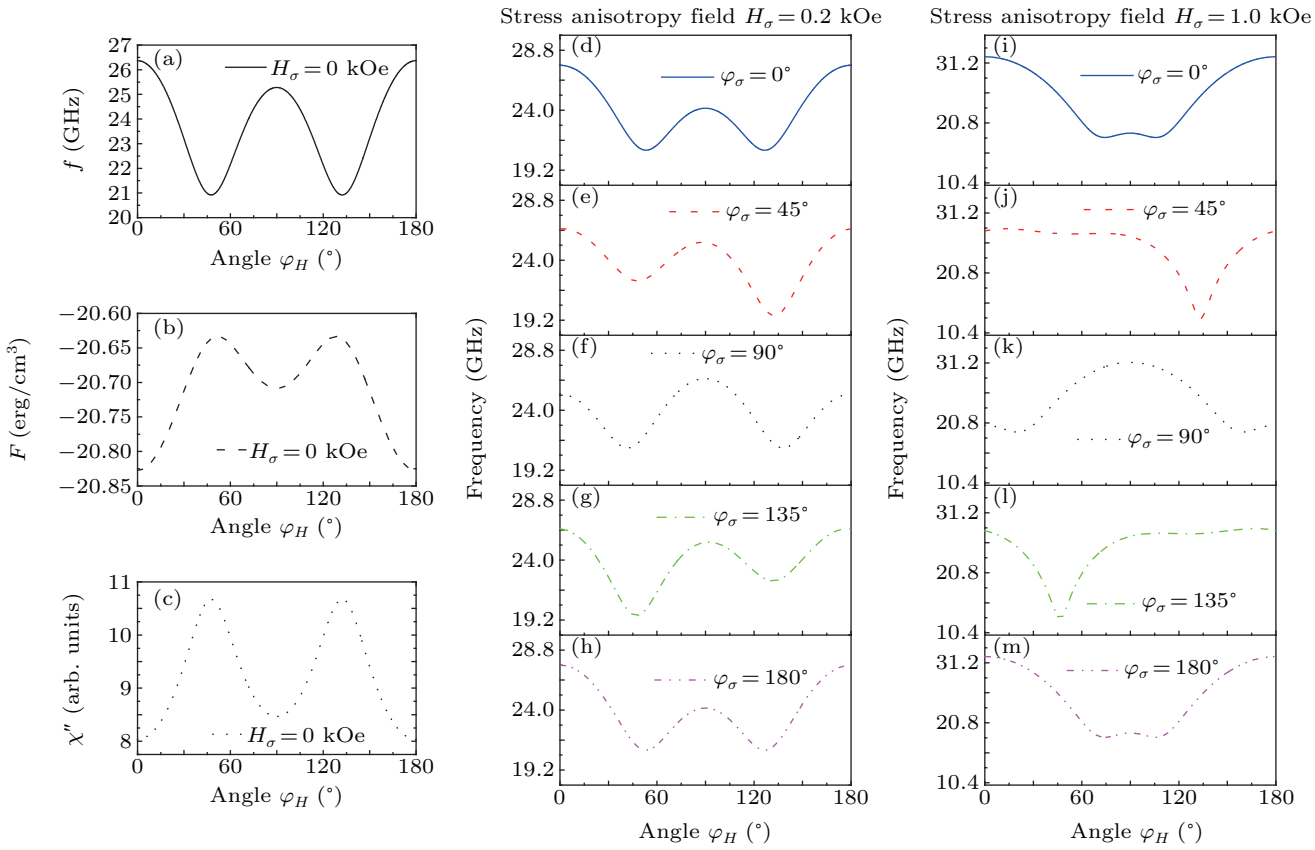


Fig. 3. Direction of the applied magnetic field dependence of FMR frequency, magnetic free-energy density and imaginary part of magnetic susceptibility in the absence of external stress anisotropy field (left panel). FMR frequency dependent on the direction of applied magnetic field with different directions of external stress anisotropy field: $H_\sigma = 0.2$ kOe (middle panel) and $H_\sigma = 1.0$ kOe (right panel).

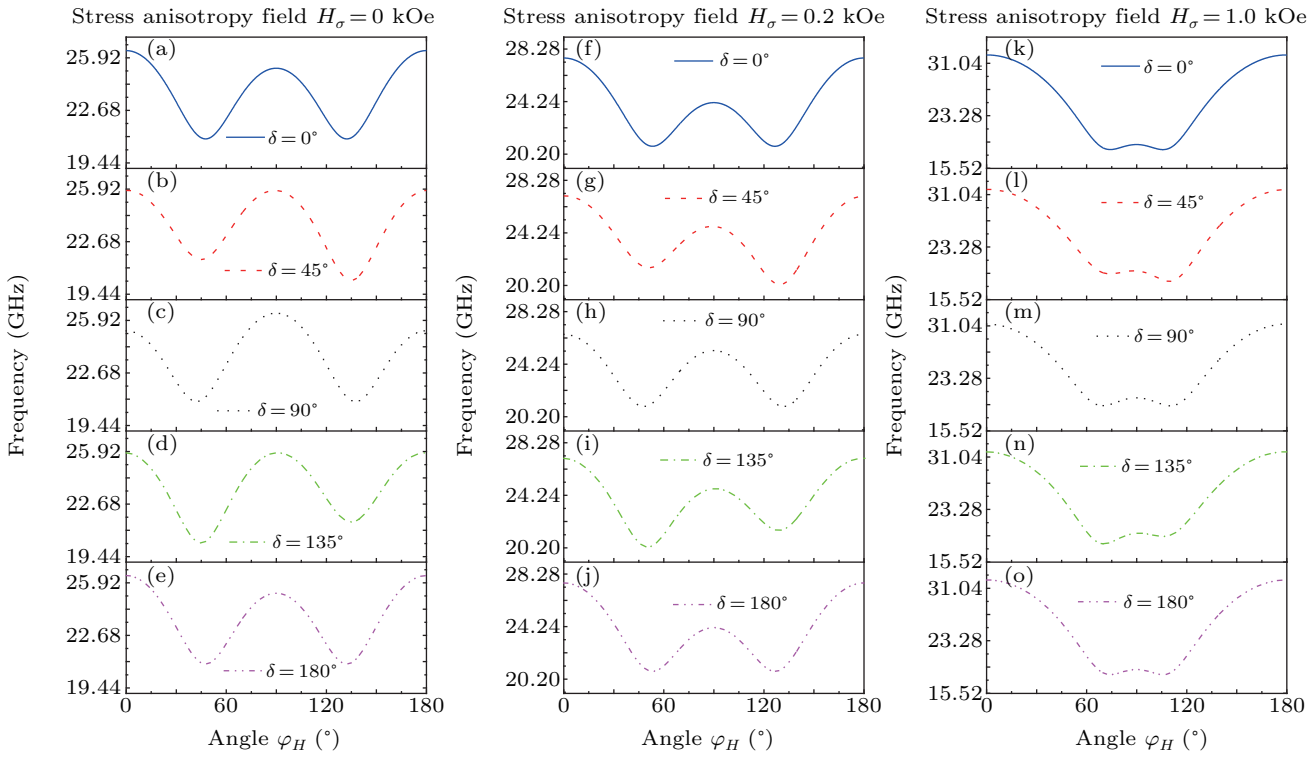


Fig. 4. FMR frequency as a function of the direction of applied magnetic field for different directions of in-plane uniaxial anisotropy field: $H_\sigma = 0$ kOe (left panel), $H_\sigma = 0.2$ kOe (middle panel), and $H_\sigma = 1.0$ kOe (right panel).

of the applied magnetic field for different in-plane uniaxial anisotropy field directions. Here, the intensity of the external stress anisotropy field is fixed at 0 kOe, 0.2 kOe, 1.0 kOe, respectively, corresponding to its direction applied along the x axis positive direction ($\varphi_\sigma = 0°$). The comparison between Figs. 4 and 5 shows that the difference between two applied magnetic field

directions corresponding to the minimum (maximum) value of the FMR frequency (imaginary part of magnetic susceptibility) is decreased with the increasing intensity of the external stress anisotropy field. In addition, both the direction of the in-plane uniaxial anisotropy field and the intensity of the external stress anisotropy field can destroy the symmetry, and change the hard and easy magnetization directions drastically. Specifically, as the intensity of the external stress anisotropy field increases, the maximum of the FMR frequency and imaginary part of magnetic susceptibility are shifted toward the higher value.

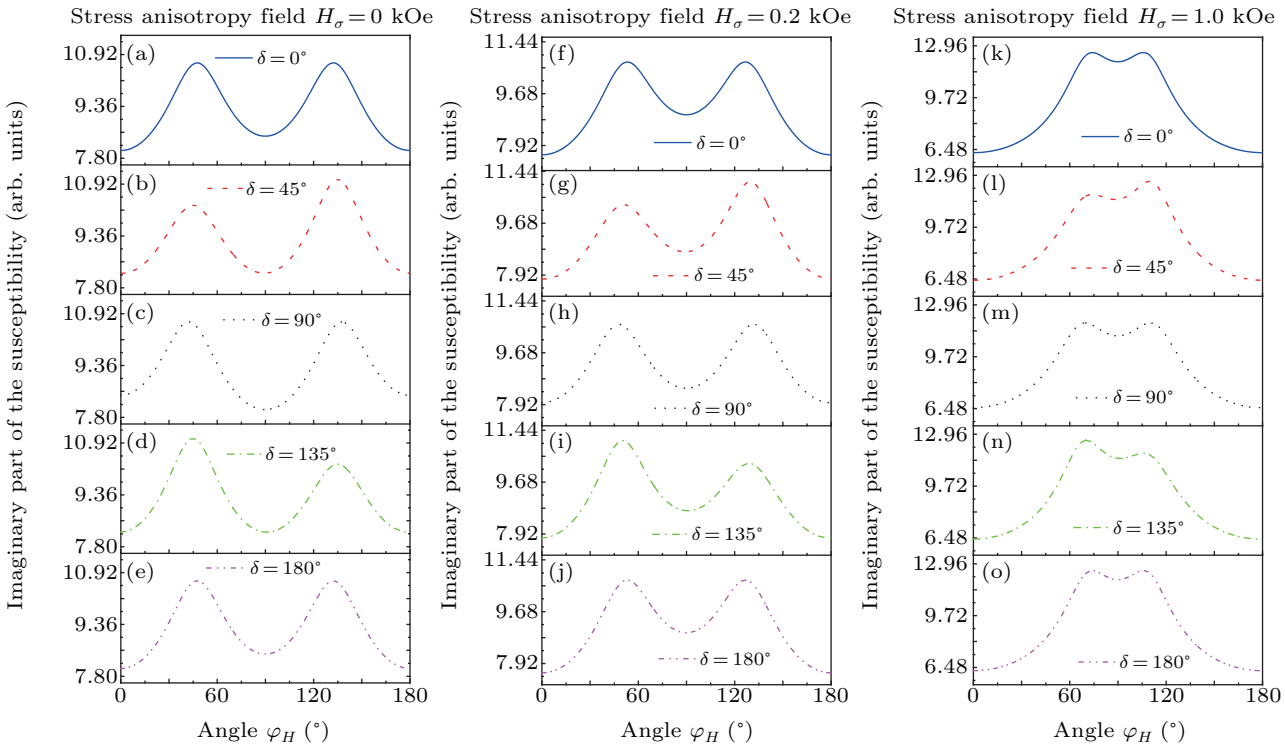


Fig. 5. Angle dependence of the imaginary part of magnetic susceptibility for different directions of the in-plane uniaxial anisotropy field: $H_\sigma = 0$ kOe (left panel), $H_\sigma = 0.2$ kOe (middle panel), and $H_\sigma = 1.0$ kOe (right panel).

3. Conclusion

In summary, the effect of the intensity of the external stress anisotropy field on a ferromagnetic thin film is obtained. It is revealed that the FMR frequency and imaginary part of magnetic susceptibility are enhanced, and the frequency linewidth or field linewidth can be broadened when the intensity of the external stress anisotropy field increases. In addition, the effects of the directions of the external stress anisotropy field and in-plane uniaxial anisotropy field are also investigated. The results show that the hard-axis and easy-axis components of magnetization strongly depend on the intensity and direction of the anisotropy field. Through comparisons, we found that it is easy to magnetize as the applied magnetic field, in-plane uniaxial anisotropy field and external stress anisotropy field are along the x axis. The intensity of the external stress anisotropy field is stronger and easier to magnetize. In short, the controllable external stress anisotropy field provides important information, which is good for applications.

Acknowledgments

Project supported by the Natural Science Foundation of Inner Mongolia of China (Grant No. 2019MS01021), the Research Program of Science and Technology at Universities of Inner Mongolia Autonomous Region, China (Grant No. NJZY21454), and the National Natural Science Foundation of China (Theoretical Physics) (Grant No. 11947414).

References

[1] Meckenstock R, Spoddig D, Himmelbauer K, Krenn H, Doi M, Keune W, Frait Z and Pelzl J 2002 *J. Magn. Magn. Mater.* **240** 410
[2] Hamida B A, Sievers S, Pierz K and Schumacher H W 2013 *J. Appl. Phys.* **114** 123704
[3] Kumar R, Samantaray B and Hossain Z 2019 *J. Phys.: Condens. Matter.* **31** 435802
[4] Wu S, Abe K, Nakano T, Mewes T, Mewes C, Mankey G J and Suzuki T 2019 *Phys. Rev. B* **99** 144416
[5] Seemann K 2021 *J. Magn. Magn. Mater.* **529** 167850
[6] Rodríguez-Suárez R L, Oliveira A B, Estrada F, Maior D S, Arana M, Santos O A, Azevedo A and Rezende S M 2018 *J. Appl. Phys.* **123** 043901
[7] Rezende S M, Azevedo A, Lucena M A and de Aguiar F M 2001 *Phys. Rev. B* **63** 214418
[8] Rezende S M, Lucena M A, Azevedo A, de Aguiar F M, Fermin J R and Parkin S S P 2003 *J. Appl. Phys.* **93** 7717
[9] Lee H, Wang Y H A, Mewes C K A, Butler W H, Mewes T, Maat S, York B, Carey M J and Childress J R 2009 *Appl. Phys. Lett.* **95** 082502
[10] Mohammadi J B, Jones J M, Paul S, Khodadadi B, Mewes C K A, Mewes T and Kaiser C 2017 *Phys. Rev. B* **95** 064414
[11] Wei Y J, Akansel S, Thersleff T, Harward I, Brucas R, Ranjbar M, Jana S, Lansaker P, Pogoryelov Y, Dumas R K, Leifer K, Karis O, Åkerman J, Celinski Z and Svedlindh P 2015 *Appl. Phys. Lett.* **106** 042405

[12] Chen H, Chen Y P, Wang T, Xie Y S, Franco A F and Xiao J Q 2020 *IEEE Trans. Magn.* **56** 2800506
[13] Mizukami S, Ando Y and Miyazaki T 2001 *J. Magn. Magn. Mater.* **226–230** 1640
[14] Sossmeier K D, Beck F, Gomes R C, Schelp L F and Cararaetc M 2010 *J. Phys. D: Appl. Phys.* **43** 055003
[15] Wang J, Tu H Q, Liang J, Zhai Y, Liu R B, Yuan Y, Huang L A, Liu T Y, Liu B, Meng H, You B, Zhang W, Xu Y B and Du J 2020 *Chin. Phys. B* **29** 107503
[16] Wang C L, Zhang S H, Li S D, Du H L, Zhao G X and Cao D R 2020 *Chin. Phys. B* **29** 046202
[17] Layadi A 2012 *J. Appl. Phys.* **112** 073901
[18] Zhang L, Rong J H, Yun G H, Wang D and Bao L B 2016 *Mater. Res. Express* **3** 076101
[19] Gandhi A C and Lin J G 2017 *J. Phys.: Condens. Matter.* **29** 215802
[20] Rong J H, Zhang L, Yun G H and Bao L B 2019 *Indian J. Phys.* **93** 207
[21] Choi S, Bac S K, Liu X Y, Lee S, Dong S, Dobrowolska M and Furdyna J K 2019 *Sci. Rep.* **9** 13061
[22] Huang Y, Wang X Q, Wu H L, Li X L, Feng H M, Liu Y Y, Liu W S, Ma Y X, Liu Q F and Wang J B 2020 *J. Magn. Magn. Mater.* **494** 165756
[23] Wang C M, Zhang S H, Huang Y C, Sang T, Cao D R, Wang X, Xu J, Zhao G X, Wang C L and Li S D 2021 *J. Magn. Magn. Mater.* **527** 167801
[24] Sipeky A and Ivanyi A 2006 *Phys. B* **372** 177
[25] Gueye M, Zighem F, Belmeguenai M, Gabor M, Tiusan C and Faurie D 2016 *J. Phys. D: Appl. Phys.* **49** 265001
[26] Li S D, Miao G X, Cao D R, Li Q, Xu J, Wen Z, Dai Y Y, Yan S S and Lu Y G 2018 *ACS Appl. Mater. Interfaces* **10** 8853
[27] Wang H, Rong J H, Yun G H and Bao L B 2019 *Acta. Phys. Pol. A* **136** 405
[28] Wang H, Zhou J Y, Wang Y N and Ma R J 2020 *Indian J. Phys.* **95** 2359
[29] Layadi A 2020 *J. Appl. Phys.* **127** 223907
[30] Smit J and Beljers H G 1955 *Philips Res. Rep.* **10** 113
[31] Suhl H 1955 *Phys. Rev.* **97** 555
[32] Celinski Z, Urquhart K B and Heinrich B 1997 *J. Magn. Magn. Mater.* **166** 6
[33] Toliński T, Lenz K, Lindner J, Kosubek E, Baberschke K, Spoddig D and Meckenstock R 2003 *Solid State Commun.* **128** 385